An Experimental and Computational Study of Solvent Effects in Toluene Chlorination

Mang Zhang and Carl R. F. Lund*

Chemical Engineering Department, University at Buffalo (SUNY), Buffalo, New York 14260-4200

Received: February 7, 2002; In Final Form: July 30, 2002

The rate of the uncatalyzed chlorination of toluene by molecular chlorine was studied without added solvent and in acetic acid solution. During competitive reaction in acetic acid, the chlorination of C_7H_8 proceeded at a rate equal to that of C_7D_8. The rate of reaction was estimated to be smaller by a factor of 10^{-4} when no solvent was added. Calculations using density functional theory suggest that the reaction is bimolecular and does not involve an arenium cation as an intermediate when low-dielectric solvents are used. The carbon−hydrogen bond is broken late in the reaction process, consistent with the observed kinetic isotope effect. The difference between the reaction rate without solvent and that in acetic acid can be attributed to the stabilization of the activated complex in acetic acid solution. The computational results suggest that in other solvents, with higher dielectric constants, the accepted reaction pathway involving an arenium cation is likely to predominate.

Introduction

Electrophilic substitution on aromatics in general, and the chlorination of toluene in particular, is a well-studied process. Nonetheless, there are aspects of toluene chlorination that are not fully explained. These include the marked effect of solvent upon reaction rate as well as the mechanism of autocatalysis by the HCl product. The present experimental and computational investigation was undertaken in order to probe the role of the solvent during the uncatalyzed chlorination of toluene. Specifically, the reaction kinetics have been studied experimentally both in acetic acid solution and without solvent, and density functional theory (DFT) calculations have been performed to probe the structure of important intermediates and the energetics of possible reaction pathways.

The chlorination of toluene by electrophilic substitution in acetic acid produces *ortho*-chlorotoluene (OCT) and *para*-chlorotoluene (PCT) as the predominant products.[1] In commercial practice, the reaction is catalyzed by a homogeneous Lewis acid catalyst, typically iron chloride, perhaps with added co-catalysts.[2−13] It appears to be generally accepted that the rate-limiting step in the reaction is the formation of an arenium cation from the reactants, Scheme 1. For example, March[14] notes that "the electrophile attacks in the first step giving rise to a positively charged intermediate (the arenium ion), and the leaving group departs in the second step...[and] for reactions in the absence of a catalyst, the attacking entity is simply Br_2 or Cl_2 that has been polarized by the ring." March[14] goes on to state that the primary evidence for the arenium cation mechanism lies in two observations. The first is the observation of a kinetic isotope effect of near unity when hydrogen is replaced by deuterium. The other is the isolation of arenium cations during the reaction of larger, highly substituted aromatics. Of course, the kinetics of the reaction are also consistent; the reaction has been observed to be first order with respect to the aromatic and first order with respect to chlorine.

The kinetics have been measured in a number of solvents, and they have commonly been quantified in terms of the apparent second-order rate coefficient at 25 °C. The results from several studies are plotted as filled circles in Figure 1 as a function of the dielectric constant of the solvent employed. The figure shows a variation in the rate coefficient of over 7 orders of magnitude. While it has been noted that the rate of reaction is affected by the polarizing ability of the solvent, see for examlple refs 15 and 16, the range of variation exhibited in Figure 1 has not been explained, nor have the trends with increasing dielectric (i.e., it is not a simple proportionality). Andrews and Keefer[15] also suggested a catalytic role for the solvent. Relatively fewer studies have additionally measured the apparent activation energy for the reaction. Still, Table 1 shows that the apparent activation energy also varies with solvent dielectric constant.

SCHEME 1

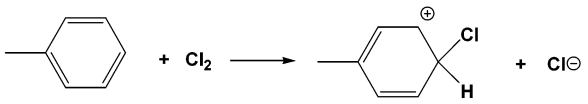

TABLE 1: Apparent Activation Energies for the Chlorination of Toluene in Various Solvents

reference	solvent	ϵ^a	E_A (kJ mol^{-1})
16	acetic acid	6.19	54.4
this work	acetic acid	6.19	53.6
16	acetic anhydride	19.44	38.1
16	acetonitrile	37.5	33.1
16	nitromethane	39.4	23.4
28	acetic acid + water + HCl		36.8

[a] Solvent dielectric constant.

A few additional points are significant. First, in a typical data analysis the second order rate expression is substituted into a mole balance for the reactor and the resulting equation is integrated. This yields an equation that can be rearranged in the form of a straight line through the origin, with the slope determining the value of the rate coefficient. Clearly, two experiments conducted at the same temperature and in the same solvent should yield the same value for the rate coefficient. Contrary to this expectation, when experiments are conducted

* Corresponding author: lund@eng.buffalo.edu, voice: (716) 645-2911 ext. 2211, fax: (716) 645-3822.

10.1021/jp0203651 CCC: $22.00
Published on Web 09/28/2002

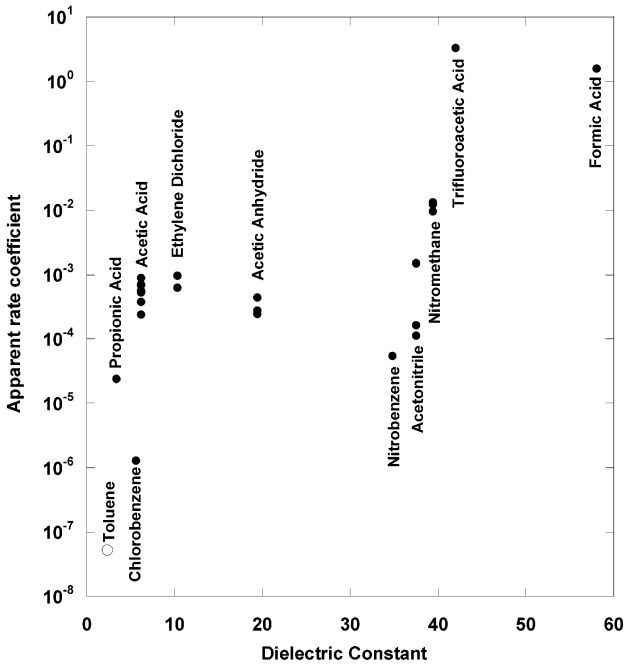

Figure 1. Reported 298 K second-order rate coefficients (L mol^{-1} s^{-1}) for toluene chlorination [refs 1, 16, 17, 19, 20, 27 and 28], filled circles, as a function of the dielectric constant of the solvent employed; the value for toluene is from the present study and corresponds to a temperature of 323 K.

SCHEME 2

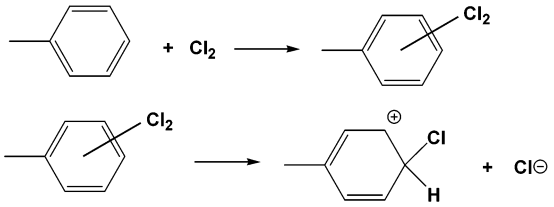

in the same solvent and at the same temperature, differing only in the initial concentrations of the reactants, the obtained rate coefficient depends on these initial concentrations, even though each of the experiments is reported to yield a straight line plot.[17] This is apparent in Figure 1 where there are several points plotted for some of the solvents. El-Dusouqui et al.[17] offered a quantitative explanation for this observation. They postulated that the reactants produce a π-complex in an equilibrated first step that is followed by a rate-determining first-order reaction of that π-complex to yield an arenium cation, Scheme 2. By assuming that iodometric titration of chlorine detects the total chlorine (free plus complexed), they were able to extract the equilibrium constant for complex formation and the rate coefficient for its further reaction from the original apparent second-order rate coefficient. El-Dusouqui et al.[17] reported that this analysis yielded a first-order rate constant (for the decomposition of the π-complex yielding an arenium cation) that did not depend on the initial concentrations of the reactants.

The other significant point about the kinetics involves autocatalysis. Smirnov et al.[18] studied chlorination in neat toluene but with added HCl. The range of concentrations of the latter extended to the liquid phase where it was effectively the solvent for the reaction. It was shown that at lower concentrations the reaction rate is proportional to toluene, chlorine, and HCl concentrations. HCl is apparently a very good catalyst; the kinetics were studied in the 170 to 230 K temperature range. At higher concentrations of HCl, the rate increases more rapidly than first order. Similarly, autocatalysis has been reported for reaction in ethylene dichloride.[16] It appears that HCl exerts virtually no effect in chlorobenzene, a slight effect in acetic acid, acetonitrile, acetic anhydride and nitromethane, and a strong effect in nitrobenzene and ethylene dichloride.[16,19] Autocatalysis was not mentioned in a report utilizing propionic, formic, and trifluoroacetic acids as solvents.[20]

Experimental Section

A 100 mL, Pyrex, round-bottomed flask served as the reactor. An electrically driven stirring rod with a paddle entered the flask through one port on the flask, and a cold-water condenser was fitted to a second port to reduce the loss of volatile components. Additional ports were available that could be used to insert a thermometer, a gas purge tube, or a sampling septum; unused ports were filled with plugs. Before each experimental run, the reactor and its miscellaneous parts were washed and subsequently rinsed with distilled water. They were then dried at 393 K for at least 12 h. Chlorine (ultrahigh purity, Matheson) was dissolved in acetic acid solution (trace metal grade, 99.5%, Fisher Scientific) until the latter was saturated, at which point the container was sealed. The reactor was charged with 90 mL of acetic acid that did not have any chlorine dissolved in it. The reactor was immersed in an isothermal water bath at the desired reaction temperature. An amount of toluene (anhydrous, 99.8%, Aldrich), 1 to 4 mL, and/or toluene-d_8 (99 atom % D, Aldrich) was added, and stirring was initiated. After the temperature stabilized, the lights were extinguished and 10 mL of the chlorine/acetic acid solution was transferred to the reaction system, starting the reaction. At measured times, samples were withdrawn from the reactor. A sampling consisted of two (20−100 μL) samples (A) taken via a 100 μL pipet to be titrated for chlorine concentration, and one (200−400 μL) sample (B) taken via a 1000 μL pipet for GC analysis of the organic components. Total sampling time was generally less than 30 s; sampling intervals were of the order of 20 min. A second, similar flask was also present in the constant temperature bath. This flask was used to measure the rate of loss of chlorine due to its volatility. It was charged and sampled in the same manner and at the same times as the reaction vessel, with the exceptions that toluene was not added and therefore only the (A) samplings were withdrawn during the course of the experiment.

Each of the A samples was mixed with 25 mL of 5% w/v potassium iodide solution (Fisher Scientific) and titrated for chlorine concentration using 0.001 N sodium thiosulfate (prepared by dilution of 0.1 N volumetric standard solution (Aldrich)) in 5 mL microburets with starch solution (Fisher) as indicator. Sample B for GC analysis was injected immediately into a quench solution vial and shaken vigorously. The quench solution consisted of 2 mL hexane (anhydrous) and 2 mL of a base solution made from 20 g NaOH (Fisher), 10 g $Na_2S_2O_3$ (99%, Aldrich), and 100 mL of distilled water. Molecular chlorine and hydrogen chloride in the sample reacted with the $Na_2S_2O_3$ and NaOH, and thereby were separated into the aqueous phase. The organic phase could then be analyzed via gas chromatography after the completion of the kinetic run. It was determined in separate experiments that the quench solution was effective by noting that the composition of the organic phase remained unchanged up to 72 h after the quench.

An SRI model 8610B gas chromatograph (GC) equipped with a flame ionization detector was used to analyze the organic fraction of the quenched reactor samples. The GC was equipped with a 28 m Alltech Econo-Cap capillary column with a 0.53

SCHEME 3

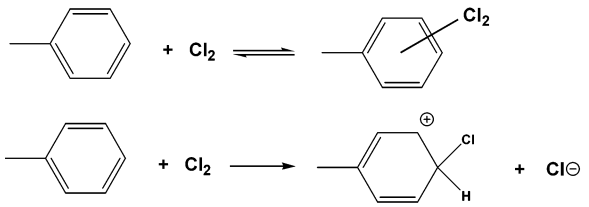

mm inner diameter and a 1.2 μm thick film of Alltech's SE-54 stationary phase. Helium (Cryogenic, high purity grade) was used as the carrier gas. A 10 μL syringe was used to inject 0.5 μL of the organic phase. The injector temperature was 50 °C, and the column temperature was programmed for the analysis as follows: hold at 50 °C for 5 min (hexane and toluene are eluted), ramp at 2 °C per min to 60 °C (monochlorotoluenes are eluted), ramp at a rate of 20 °C per min to 200 °C, and hold 8 min (benzyl chloride and dichlorotoluenes, if present, are eluted). It should be noted that in most cases neither benzyl chloride nor any dichlorotoluene was detected. The GC was calibrated immediately before or after each experiment by injecting different amounts of samples of three solutions with known composition of toluene, *para*-chlorotoluene (99%, Aldrich), *ortho*-chlorotoluene (98%, Aldrich), benzyl chloride, etc. Data acquisition was performed using Peaksimple v1.23 with a sampling rate of 1 Hz.

Kinetic experiments, as just described, were conducted at temperatures of 303, 313 and 323 K. A run was also made using no solvent at 323 K. Of course, it was not possible to perform a separate, parallel volatility loss experiment. The run was allowed to proceed for 19 h, at which time the amount of chlorinated product was approximately equal to the amount after 1 to 2 min in the presence of acetic acid. To investigate the kinetic isotope effect, competitive chlorination at 303 K was used. Equal amounts of C_7H_8 and C_7D_8 were charged to the reactor at the start of a kinetic run. Chlorine concentration was determined as previously described. In this case, the quenched organic phase from the reactor sampling was analyzed by GC-MS.

The structure and energetics of reactants, products, and intermediates were calculated using Jaguar, version 4.0.[21] Except where noted otherwise, density functional theory (DFT) was employed using B3LYP hybrid exchange and correlation functionals and a cc-pvtz(-f) basis set. Fine DFT grids were employed, and ultrafine geometry convergence was specified. The polarized continuum model for solvation[22] that is included in the Jaguar program was used when optimizing structures and calculating energetics in solution. Partial atomic charges were calculated by fitting the electrostatic potential to the atom centers while constraining the total charge to equal that of the species. Neither frequencies nor zero-point energies were scaled. Molden[23] was used for visualization of molecular orbitals.

Results

A number of precautions must be taken in the analysis of the experimental kinetic data. First, chlorine can be lost from the reactor due to its volatility. Thus, the decrease in the chlorine concentration during an experiment is due only in part to its consumption by the reaction. Second, it has been proposed that π-complexes form between toluene and chlorine. This might occur as a first step in the reaction mechanism, Scheme 2, or as a parallel process, Scheme 3. In either case, if a π-complex does form, before relating the measured concentrations to the kinetics, one must determine whether the analytical procedures measure the free chlorine or the total (free plus complexed) chlorine concentration, and similarly, whether they measure the free toluene or the total toluene concentration. Third, for some systems autocatalysis by HCl has been reported, and if this effect is important, it must also be incorporated in the kinetic analysis. It appears that most of the early studies took precautions to minimize the loss of chlorine due to volatilization, and then ignored the small residual loss during the kinetic analysis. It also appears that apart from El-Dusouqui et al.,[17] the kinetic analysis used in most studies has not considered the possibility of π-complex formation, and consequently the measured chlorine has been assumed to be free chlorine. Finally, prior studies have typically ignored the autocatalytic effect of HCl unless it imparted observable nonlinearity into the second-order kinetic analysis.

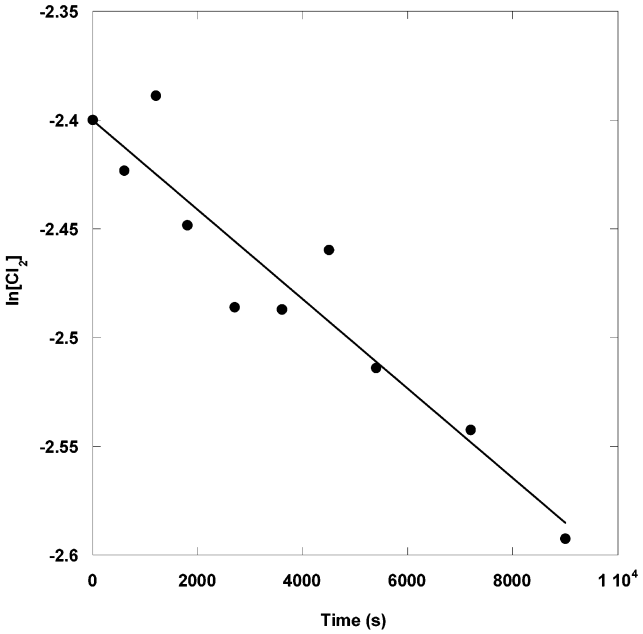

Figure 2. Typical fit (line) of first-order kinetics to the measured chlorine concentration data (circles) from the chlorine loss experiments.

In the present investigation, only a few kinetic runs have been made. To ensure as meaningful a comparison to prior work as possible, the kinetic analysis ignored any possible autocatalytic effect of HCl, and it assumed that π-complex concentrations could be ignored. However, the experimental results showed that chlorine loss due to volatilization was significant. To account for this phenomenon, the kinetic experiments in acetic acid solution were paralleled by identical experiments, except for the absence of toluene. The data from these parallel experiments consisted of concentrations of dissolved chlorine versus time. These data were analyzed assuming chlorine volatilization to be represented by a first-order process. Typical results, for the run at 303 K, are shown in Figure 2, where the measured chlorine concentrations are plotted along with the concentrations predicted by the first-order fit.

Letting C_L denote the total moles of chlorine lost via volatilization divided by the total fluid volume, C denote the dissolved chlorine concentration, C_T^0 and C^0 denote the initial toluene concentration and chlorine concentrations, k denote the second-order rate coefficient for the chlorination reaction, and k_v denote the apparent first-order rate coefficient for the volatilization process, the mole balance equations for chlorine are given by eqs 1 and 2. In deriving these equations it has been assumed that the production of benzyl chloride and polychlorinated toluenes is negligible (consistent with experi-

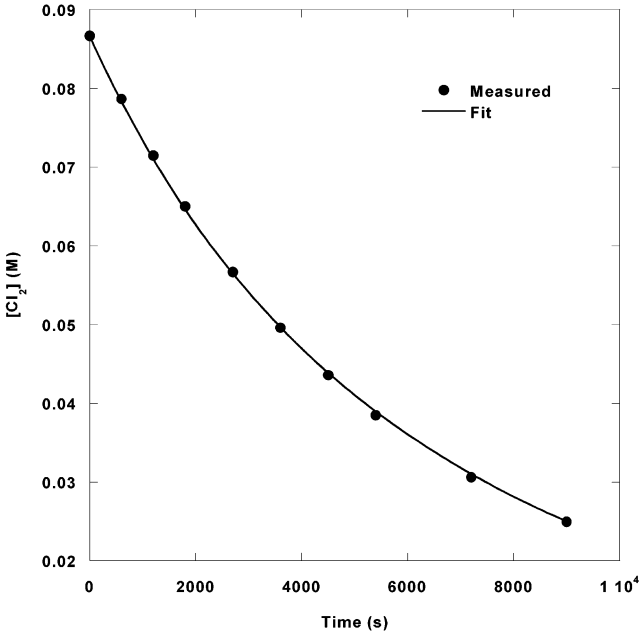

Figure 3. Comparison of the chlorine concentration versus time predicted by the second-order kinetic fit (line) to the experimental data (circles) for the experiment at 303 K.

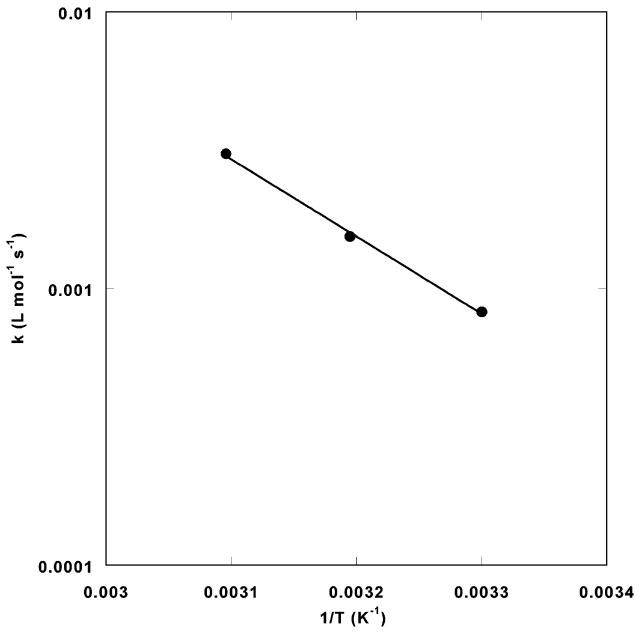

Figure 4. Arrhenius plot of the second-order rate coefficients for toluene chlorination in acetic acid.

mental observation). Initially, at $t = 0$, no chlorine has been lost, so $C_L = 0$, and $C = C^0$. These equations were fit to the experimental data for each temperature using the Athena Visual Workbench program.[24] Figure 3 presents a typical result for the data at 303 K, comparing the measured chlorine concentration versus time to that predicted using the fitted equations.

$$\frac{dC}{dt} = -k_v C - kC(C_T^0 - C^0 + C - C_L) \qquad (1)$$

$$\frac{dC_L}{dt} = k_v C \qquad (2)$$

The same kinetic analysis was applied using the data for experiments at temperatures of 313 and 323 K. An Arrhenius plot of the resulting rate coefficients is shown in Figure 4. The corresponding expression for the rate coefficient is given in eq 3. As a check on the experimental procedure and results, eq 3 was used to calculate the expected value of the rate coefficient at 298 K. The resulting value, 5.67×10^{-8} L mol^{-1} s^{-1}, is in excellent agreement with the values reported in the literature. (Reference to Figure 1 shows that this value is within the range of values reported previously by other investigators.) An Eyring plot of the data (not shown) gave a value of 50.8 kJ mol^{-1} for the enthalpy of activation.

$$k = \left(1.32 \times 10^6 \frac{\text{L}}{\text{mol s}}\right) \exp\left(\frac{-53.6 \text{ kJ mol}^{-1}}{RT}\right) \qquad (3)$$

The rate of reaction in neat toluene was very much slower than the rate in acetic acid. In fact, the decrease in chlorine concentration with time was approximately equal to that due to volatilization from acetic acid. Because it was not possible to separately measure the volatilization from toluene, the rate was instead estimated from the concentration of chlorinated products at the end of the experiment. Using the initial chlorine and toluene concentrations, it was estimated that the rate of reaction in neat toluene was approximately 10^{-4} times the rate in acetic acid solution and that the rate coefficient was equal to 5.3×10^{-8} L mol^{-1} s^{-1} at 323 K. This value is included for comparison as an unfilled circle in the plot of Figure 1; of course, the value at 298 K would be expected to be smaller.

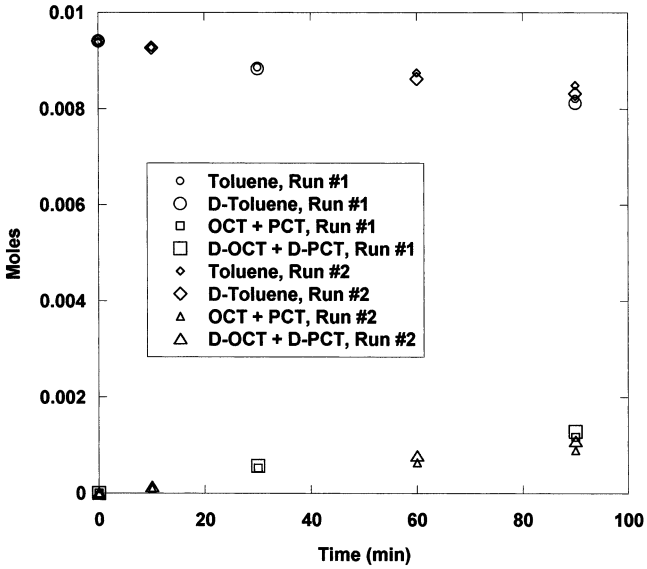

Figure 5. Variation in concentrations of labeled and unlabeled toluene and total chlorotoluenes during the competitive chlorination of C_7H_8 and C_7D_8 at 303 K.

Insufficient data were collected during the competitive chlorination of C_7H_8 and C_7D_8 to permit a rigorous kinetic analysis. Instead, Figure 5 shows how the labeled and unlabeled toluene and total chlorotoluenes varied during the two runs. It is clear from the data that the rates are identical to within the limits of experimental error. A measurable kinetic isotope effect would have manifested itself in unlabeled product concentrations that increased faster than the labeled product concentrations, and unlabeled toluene concentrations that decreased faster than the labeled toluene concentrations.

The computational analysis began with consideration of the stable reactants and products of the chlorination reaction: Cl_2, C_7H_8, *o*-C_7H_7Cl, *m*-C_7H_7Cl, *p*-C_7H_7Cl, and HCl. For each of these species the structures were optimized and the resulting energies were determined. Following this, a vibrational analysis

TABLE 2: Calculated Energies of Relevant Species in Different Solvents

	gas phase		toluene		acetic acid		nitromethane	
reagents	energy[a]	ZPE[b]	energy[a]	ZPE[b]	energy[a]	ZPE[b]	energy[a]	ZPE[b]
Cl_2	−920.42993	3.473	−920.429929	3.163	−920.429929	3.163	−920.429929	3.163
C_7H_8	−271.65459	335.2	−271.656774	334.2	−271.658362	335.0	−271.659446	335.0
o-C_7H_7Cl	−731.28484	311.1	−731.287008	310.1	−731.288541	309.6		
m-C_7H_7Cl	−731.28488	310.2	−731.287222	309.2	−731.288833	308.9		
p-C_7H_7Cl	−731.2846	310.1	−731.286992	309.1	−731.288576	309.4	−731.286961	309.0
HCl	−460.84152	17.53	−460.843483	17.41	−460.845017	17.29	−460.845389	17.26
			Intermediates					
p-$C_7H_8Cl^+$	−731.57904	338.0	−731.630309	338.5	−731.654238	338.6	−731.667357	337.9
Cl^-	−460.29752	0.0	−460.372596	0	−460.405895	0	−460.423776	0
			Activated Complex					
p-$C_7H_8Cl_2$	−1192.0168	340.7	−1192.039190	339.4	−1192.064401	339.0		

	nitrobenzene		acetonitrile		acetic anhydride		chlorobenzene	
reagents	energy[a]	ZPE[b]	energy[a]	ZPE[b]	energy[a]	ZPE[b]	energy[a]	ZPE[b]
Cl_2	−920.429929	3.163	−920.429929	3.163	−920.429929	3.163	−920.429929	3.163
C_7H_8	−271.659389	334.8	−271.659416	334.9	−271.659217	334.8	−271.658240	334.9
			Intermediates					
p-$C_7H_8Cl^+$	−731.666834	336.5	−731.667248	337.6	−731.664719	336.4	−731.652865	337.5
Cl^-	−460.423433	0	−460.423607	0	−460.420537	0	−460.404265	0
			Activated Complex					
p-$C_7H_8Cl_2$								

[a] Electronic energy plus nuclear repulsion, Hartrees. [b] Unscaled zero-point energy, kJ mol^{-1}.

was performed on the minimum-energy structure. The frequencies were checked to make sure that all were real, and the zero-point energy was determined. Neither the vibrational frequencies nor the zero point energies were scaled. This set of calculations was performed for the species in the gas phase, in toluene solution and in acetic acid solution. In addition, the calculations were also performed for the reactants (Cl_2 and C_7H_8) in nitromethane, nitrobenzene, acetonitrile, acetic anhydride, and chlorobenzene. The energy results from all these calculations are shown in Table 2.

It appears to be generally accepted[14,25,26] that the rate-limiting step in the chlorination of aromatics involves the formation of an arenium cation as a reaction intermediate. Hence similar calculations were performed on *p*-$C_7H_8Cl^+$ and Cl^- in the gas phase and in all of the same solvents. The energy results are included in Table 2. Finally, an attempt was made to locate transition states that connected the reactants either to the arenium cation/chloride anion intermediates or directly to the *p*-chlorotoluene/HCl products. In most instances, these attempts failed, and transition states were not located. However, for the gas phase and in solutions of toluene and acetic acid, transition states connecting the reactants and the products (i.e., without an arenium cation intermediate) were identified. The resulting structure of the activated complex corresponding to the gas phase transition state for direct reaction of the reactants to the products is shown in Figure 6a, and the energies are again included in Table 2.

Discussion

Figure 1 shows that the rate of toluene chlorination initially increases sharply with the dielectric constant of the solvent. Henceforth this will be referred to as the low dielectric regime. Then, in the vicinity of a dielectric constant of 10, the trend changes, and the rate of reaction becomes much less sensitive to the dielectric constant of the solvent. This will be referred to as the intermediate dielectric regime. At a dielectric constant around 40 there is a second regime where the rate increases sharply with the dielectric, and this is followed by a second plateau regime above ca. 40. The focus of the present work is in the low and intermediate dielectric regimes, and in particular, on the transition between these two regimes. It can be seen that of the experimentally studied systems, chlorination in toluene falls in the low dielectric regime while that in acetic acid falls in the region of transition between the two regimes. The systems that have been investigated computationally span the range from the low dielectric regime through the transition and into the intermediate dielectric regime.

As noted in the Introduction, uncatalyzed chlorination has been studied in a number of solvents. The rate coefficient for reaction in acetic acid derived in the present investigation is in excellent agreement with the previous work, as is the measured activation energy (see Table 1). The rate coefficient for the uncatalyzed reaction without solvent (at 323 K) was also experimentally estimated and is plotted in Figure 1; the authors are not aware of any other reported values that can be used for comparison. It was also noted in the Introduction that the primary evidence for the arenium ion mechanism in general involves the kinetic isotope effect and the isolation of arenium cations. The present authors are not aware of measurements of the kinetic isotope effect for toluene chlorination in the low and intermediate dielectric regime. In trifluoroacetic acid (high dielectric regime) a primary kinetic isotope effect was not observed by Himoe and Stock.[20] The kinetic isotope effect measured during competitive chlorination of toluene in this study is essentially unity, consistent with this result.

The computational results from Table 2 were used to calculate ΔE_0, the change in energy (including zero point energies), for the formation of a *para*-chlorotoluene arenium cation and a chloride anion from toluene and chlorine. The results are shown in Table 3. The wide and systematic variation in the energetics, as discussed presently, suggest that the simple polarized continuum model for solvation is sufficient to capture many of the important features of these reaction systems. In the intermediate dielectric regime, the calculations predict that the arenium cation and chloride anion are more stable than the reactants in nitrobenzene, nitromethane and acetonitrile. In acetic

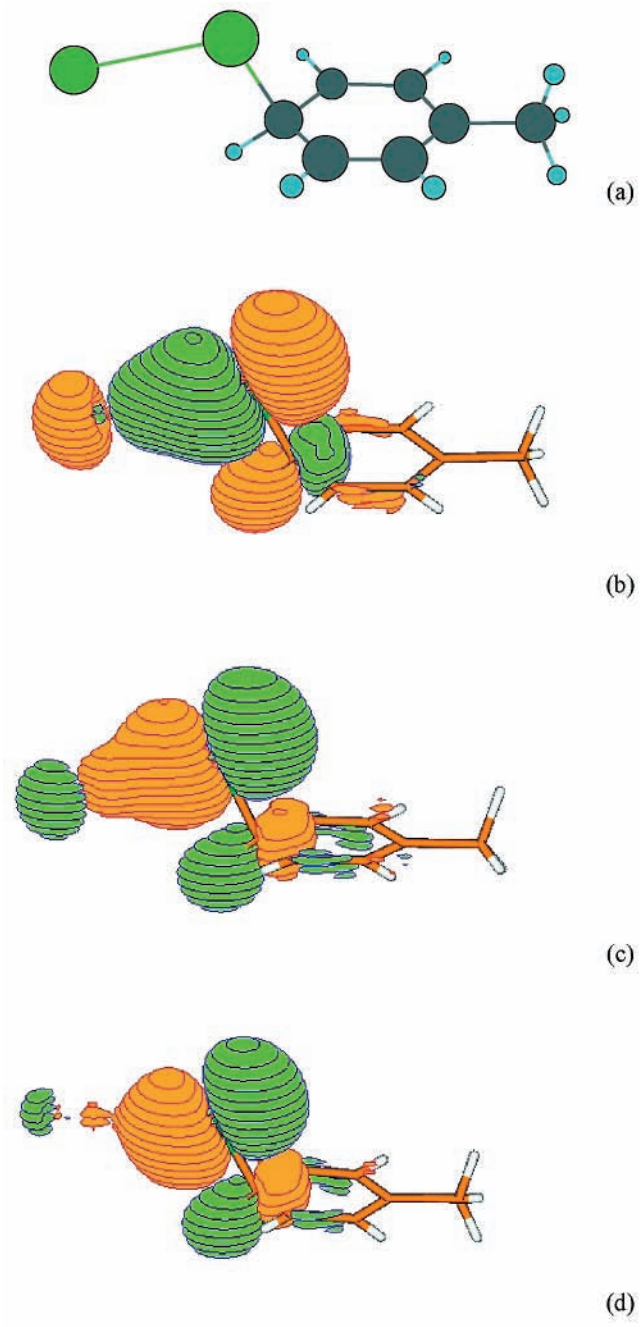

Figure 6. Geometry of the gas phase activated complex (a) and one of its molecular orbitals (b) suggesting a chlorine−chlorine bond that gradually disappears as the solvent changes to toluene (c) and acetic acid (d).

anhydride, the calculated energy for formation of these ions is lower than the experimentally determined activation energy. That is, in the intermediate dielectric regime, the computational results are consistent with the accepted mechanism for the reaction wherein the rate-limiting step is the formation of an arenium cation from the reactants. Many attempts were made to identify transition states for the formation of the arenium cation in the solvents of the intermediate dielectric regime, but without success. Therefore, it was not possible to compare calculated barriers to the experimental data. In short then, the computational results indicate that when the dielectric constant is greater than ca. 10, the accepted arenium cation pathway is energetically favorable. Within this regime there are still variations among the solvents, and these differences may be attributed to structural differences among the solvent molecules (aromatics vs organic acids), catalytic activity of the solvents, etc.

TABLE 3: Calculated Energetics of the Formation of an Arenium Cation and of an Activated Complex for a Direct Reaction Pathway in Various Solvents Compared to the Experimentally Measured Activation Energies from Table 1

solvent	dielectric ϵ	ΔE_0 (kJ mol^{-1}) $C_7H_8 + Cl_2 \rightarrow$ p-$C_7H_8Cl^+ + Cl^-$	$\Delta E_0^{\ddagger}$ (kJ mol^{-1}) $C_7H_8 + Cl_2 \rightarrow$ p-$C_7H_8Cl_2$	E_A expt. (kJ mol^{-1})
gas phase		545.97	177.80	
toluene	2.379	220.01	124.74	
chlorobenzene	5.708	81.49		
acetic acid	6.15	73.93	62.72	53.6−54.4
acetic anhydride	20	10.21		38.07
nitrobenzene	34.82	−2.49		
acetonitrile	37.5	−3.96		33.05
nitromethane	39.4	−4.62		23.43

TABLE 4: Comparison of Selected Bond Lengths, Bond Angles, and Charges of the Activated Complex and the *para*-Chlorotoluene Arenium Cation in Low Dielectric Solvents

		gas phase	toluene	acetic acid
arenium cation	H−C−Cl angle	104.6	104.5	104.6
activated complex	H−C−Cl angle	99.5	102.5	104
arenium cation	C−Cl distance	1.82	1.821	1.825
activated complex	C−Cl distance	1.882	1.862	1.84
activated complex	C−Cl−Cl angle	98.8	104.2	109.3
activated complex	Cl−Cl distance	2.931	3.114	3.473
activated complex	H−Cl (terminal) distance	3.112	3.583	3.983
activated complex	charge on terminal Cl	−0.48	−0.71	−0.94

SCHEME 4

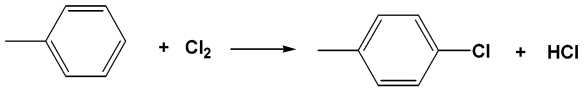

Table 3 shows different behavior in the low dielectric regime. In that regime, the energy required to form the arenium cation and chloride anion increases markedly as the dielectric constant decreases. Unfortunately, for the most part, experimental activation energies are not available for reaction in this regime. Acetic acid is in the vicinity of the transition between the two regimes. For reaction in acetic acid, the calculated energy needed to form the arenium cation and chloride anion is slightly greater than the reported activation energy for the overall reaction, but the amount is probably within the uncertainty of the calculated energies (ca. 10 kJ mol^{-1}).

The highly endothermic nature of arenium cation formation in the low dielectric regime found in the calculations suggests that there could be a different reaction pathway that does not involve an arenium cation. This prompted a search for a direct reaction pathway that does not involve forming an arenium cation, Scheme 4. The activated complex shown in Figure 6a was identified as corresponding to a gas phase transition state connecting the reactants directly to the products (i.e., without an arenium cation intermediate). Following the reaction coordinate from this transition state in one direction led to toluene and molecular chlorine, and following it in the other direction led to *p*-chlorotoluene and HCl. Similar transition state structures were found in toluene and in acetic acid solution, when the solvent was modeled as a polarized continuum. Table 4 compares selected bond lengths and angles of these activated complexes and of a *p*-chlorotoluene arenium cation in a few solvents.

The facts that the activated complexes were identified in a transition state search, that they possess a single imaginary vibrational frequency, and that following the reaction coordinate leads to either the products or the reactants suggest rather convincingly that the species shown in Figure 6a is indeed an activated complex connecting the reactants directly to the products. However, a visual inspection shows that the distance between the two chlorine atoms is quite large (2.93 to 3.47 Å; see Table 4) compared to the normal bond length in molecular chlorine, 2.04 Å. Indeed, one might argue that the structure shown in Figure 6a is actually a tightly coupled ion pair, and therefore that the arenium cation is in fact an intermediate. (It must be remembered, however, that this structure is not a minimum energy structure.) To further probe this issue, the various molecular orbitals of the activated complex were visualized. Figure 6b shows one particularly relevant orbital of the gas phase activated complex that clearly indicates bonding between the two chlorine atoms. In particular, one can see significant electron density between the two chlorine atoms in what appears to be a sigma bond formed from the p orbitals of the chlorine atoms. As reported in Table 4, the charge on the terminal chlorine atom is considerably smaller than one, as well. In short, the species shown in Figure 6a appears to be a true activated complex for a gas phase reaction pathway that leads directly from the reactants to the products without the formation of an arenium cation as an intermediate.

As mentioned in the Introduction, El-Dusouqui et al.[17] noticed that the apparent second order rate coefficients for toluene chlorination in acetic acid were dependent upon the initial concentrations of the reactants. They were able to rationalize this observation in terms of Scheme 2, which is not consistent with the computational results of the present study. The activated complex just discussed lies along a reaction pathway that directly connects the reactants to the products; it does not connect a π-complex to the products. However, the key point in the analysis of El-Dusouqui et al.[17] is that the formation of the complex reduces the concentration of free chlorine. It can be shown using the same assumptions as El-Dusouqui et al.[17] that Scheme 3 is equally capable of describing the kinetic results, and at the same time, it is consistent with the reaction pathway proposed in the present work. It was also mentioned in the Introduction that the reaction is autocatalytic. The transition state described above then must correspond to the situation where the concentration of HCl is very low, such as at the start of an experimental run. No attempt was made in the present study to identify the transition state for the HCl-catalyzed chlorination.

The computational results for different solvents can be clearly differentiated into two groups. The first group includes the gas phase, toluene solution, and acetic acid solution. In each of the systems in this group an activated complex for the direct reaction pathway was identified computationally, and for each system the associated activation energy for formation of this activated complex is less than the energy of formation of an arenium cation. Also, in the one situation where an experimental activation energy is available, acetic acid solution, the computationally predicted activation energy, 62.7 kJ mol^{-1}, agrees reasonably well with the experimentally measured values, 53.6−54.4 kJ mol^{-1} shown in Table 1. Finally, all the systems that fall into this group also appear in the low dielectric regime of Figure 1.

The second group of solvents includes acetic anhydride, acetonitrile, nitrobenzene, and nitromethane. Attempts to identify an activated complex for the direct reaction pathway failed for each of these solvents, even when the structure of the activated complex from the first group was used as an initial guess. This group is further distinguished from the first group in that the formation of an arenium cation and chloride anion is calculated to be exothermic or (for acetic anhydride) slightly endothermic, and in all cases much less than the apparent activation energy of the chlorination reaction. That is, for this group the DFT results predict facile formation of the arenium cation. This group of solvents falls in the intermediate dielectric regime of Figure 1.

The clear differentiation of the computational results into two groups that correspond directly to two different regimes of Figure 1 suggests an explanation for the gross features of that figure. The regime of low dielectric may represent a regime wherein it is very difficult to form an arenium cation, and consequently the predominant reaction pathway is a direct conversion of the reactants to the products through an activated complex similar to that shown in Figure 6. In the vicinity of the transition (dielectric $\cong$10), the energetics of arenium cation formation become favorable. Thus the transition in Figure 1 at a dielectric constant of ca. 10 may correspond to a change in the predominant reaction pathway from a direct one to one where an intermediate arenium cation is formed. Other results support this postulate as well. The molecular orbitals shown in Figure 6 show that as one moves from the gas phase to toluene to acetic acid (i.e., from the low dielectric regime toward the transition), the bonding orbital joining the two chlorine atoms "necks down." Extrapolation suggests that if the dielectric constant continued to increase, the bond would disappear. That is, an arenium cation would result. Similarly, the data in Table 4 show that again as one moves from low dielectric toward the transition, the geometric parameters of the activated complex approach those of the arenium cation. Additionally, as one moves from low to higher dielectric, the charge on the terminal chlorine of the activated complex approaches the value of −1 that would be expected for the arenium cation mechanism.

The kinetics of the reaction would be second order for each of the two pathways, Scheme 1 and Scheme 4. This is consistent with experimental observation in that the reaction order does not change between the two regimes. The absence of an apparent kinetic isotope effect is also consistent with the direct pathway, Scheme 4, when the transition state shown in Figure 6 is considered. In that figure, the carbon-to-hydrogen bond is still intact. A kinetic isotope effect different from unity would be expected only if the hydrogen/deuterium was involved in a bond that was breaking or forming in the transition state. The figure and the tracing of the reaction coordinate in this case indicate that the carbon-to-hydrogen bond breaks very late in the process, well past the transition state and consistent with the observed kinetic isotope effect.

The polarized continuum model of solvation was sufficient to uncover the gross differences in reaction pathway between the low and intermediate dielectric regimes. The reason for this is that the stability of the arenium cation is the primary difference between the two regimes. It is expected that, to explain the smaller differences within the intermediate dielectric regime, it will be necessary to consider specific solvent interactions. It seems reasonable to speculate that the second regime of increasing activity seen in Figure 1 at dielectric constants greater than ca. 40 is not a solvent effect, but a catalytic effect. That is, it is possible that the solvents begin to act as catalysts for the reaction.

Finally, before concluding, it should be noted that a series of calculations were performed using different basis sets and

TABLE 5: Calculated Energetics (kJ mol^{-1}) of Formation of the Arenium Cation and of the Activated Complex Using Different Basis Sets and Levels of Theory

		cc-pvtz(-f) b3lyp	6-31G** b3lyp	cc-pvtz(-f) mp2
$C_7H_8 + Cl_2 \rightarrow$	acetic acid	73.93	59.04	91.96
p-$C_7H_8Cl^+ + Cl^-$	toluene	220.01	206.15	233.14
$C_7H_8 + Cl_2 \rightarrow$	acetic acid	62.72	50.93	81.03
p-$C_7H_8Cl_2$	toluene	124.74	104.66	162.59

different levels of theory. These calculations were performed only for the systems in the low dielectric regime; they are summarized in Table 5. The table shows that in all cases the predicted energy for forming the activated complex is ca. 10 kJ mol^{-1} less than that for forming an arenium cation in acetic acid, and ca. 70 to 100 kJ mol^{-1} less in toluene. The predicted activation energies for reaction in acetic acid all agree reasonably with the experimental value, as well.

Conclusions

The rate of the chlorination of toluene shows a very strong dependence upon the dielectric constant of the reaction medium. For reaction in solvents of low dielectric constant, less than ca. 10, a direct pathway from reactants to products is energetically more favorable than one that involves an arenium cation as an intermediate. Experimental data for chlorination of toluene in acetic acid are consistent with this interpretation: the reaction is second order with an activation energy of 53.6 kJ mol^{-1}. No kinetic isotope effect was observed experimentally, and this, too, is consistent with the direct pathway as DFT calculations have shown that the carbon−hydrogen bond is broken quite late in the process. As the dielectric is increased further, arenium cations are stabilized, and hence become feasible as mechanistic intermediates. This suggests that the experimentally observed break (at a dielectric of ca. 10) in a plot of the rate constant versus solvent dielectric is associated with a transition from a direct pathway at low dielectric to the generally accepted arenium ion pathway at higher dielectric constants.

Acknowledgment. This material is based upon work supported, in part, by the National Science Foundation under Awards CTS-9727315 and CTS-0099359. It would not have been possible without access to the resources provided by the Center for Computational Research at the University at Buffalo, SUNY.

References and Notes

(1) Brown, H. C.; Stock, L. M. *J. Am. Chem. Soc.* **1957**, *79*, 5175.
(2) van Dijk, J.; van Daalen, J. J.; Paerels, G. B. *Recl. Trav. Chim. Pays-Bas* **1974**, *93*, 72.
(3) Suzuki, T.; Komatsu, C. Process for Producing a Halobenzene. U.S. Patent No. 4,831,199, Assigned to Ihara Chemical Industry Co., 1989.
(4) Graham, J. C. Process for the Preparation of Monochlorotoluene. U.S. Patent No. 4,013,730, Assigned to Hooker Chemicals & Plastics Corporation, 1977.
(5) Graham, J. C. Process for the Directed Chlorination of Alkylbenzenes. U.S. Patent No. 4,031,142, Assigned to Hooker Chemicals & Plastics Corporation, 1977.
(6) Graham, J. C. Process for Directed Chlorination of Alkylbenzenes. U.S. Patent No. 4,031,147, Assigned to Hooker Chemicals & Plastics Corporation, 1977.
(7) Buckholtz, H. E.; Bose, A. C. Process for the Chlorination of Toluene. U.S. Patent No. 4,024,198, Assigned to Hooker Chemicals & Plastics Corporation, 1977.
(8) Di Bella, E. P. Chlorination of Toluene. U.S. Patent No. 4,031,144, Assigned to Tenneco Chemicals, Inc., 1977.
(9) Lin, H. C. Process for Directed Chlorination of Alkylbenzenes. U.S. Patent No. 4,069,263, Assigned to Hooker Chemicals & Plastics Corporation, 1978.
(10) Lin, H. C. Process and Catalyst Mixture for the Para-Directed Chlorination of Alkylbenzenes. U.S. Patent No. 4,250,122, Assigned to Hooker Chemicals & Plastics Corp., 1981.
(11) Hattori, R.; Abe, Y.; Kanno, S.; Maeda, S. Process for the Nuclear Chlorination of Toluene. U.S. Patent No. 4,444,983, Assigned to Hodogaya Chemical Co., Ltd., 1984.
(12) Schrage, H.; Fiege, H. Process for the Nuclear Chlorination of Aromatic Hydrocarbons. U.S. Patent No. 5,315,049, Assigned to Bayer Aktiengesellschaft, 1994.
(13) Wolfram, H. Process for Ring-Chlorinating Toluene. U.S. Patent No. 4,647,709, Assigned to Hoechst Aktiengesellschaft, 1987.
(14) March, J. *Advanced Organic Chemistry Reactions, Mechanisms, and Structure*, 4th ed.; John Wiley: New York, 1992.
(15) Andrews, J. L.; Keefer, R. M. *J. Am. Chem. Soc.* **1957**, *79*, 5169.
(16) Andrews, L. J.; Keefer, R. M. *J. Am. Chem. Soc.* **1959**, *81*, 1063.
(17) El-Dusouqui, O. M. E.; Mahmud, K. A. M.; Sulfab, Y. *J. Chem. Soc., Perkin Trans. 2* **1991**, *1991*, 1167.
(18) Smirnov, V. V.; Rostovshchikova, T. N.; Tarkhanova, I. G.; Novikov, I. N.; Barabash, V. B.; Nasyr, I. A. *Kinet. Catal.* **1993**, *34*, 204.
(19) Stock, L. M.; Himoe, A. *J. Am. Chem. Soc.* **1961**, *83*, 4605.
(20) Himoe, A.; Stock, L. M. *J. Am. Chem. Soc.* **1969**, *91*, 1452.
(21) Jaguar; 3.5, 4.0 ed.; Schrodinger, Inc.: Portland, OR, 1998.
(22) Tannor, D. J.; Marten, B.; Murphy, R.; Friesner, R. A.; Sitkoff, D.; Nicholls, A.; Ringnalda, M.; Goddard, W. A., III.; Honig, B. *J. Am. Chem. Soc.* **1994**, *116*, 11875.
(23) Schaftenaar, G.; Noordik, J. H. *J. Comput.-Aided Mol. Design* **2000**, *14*, 123.
(24) Athena Visual Workbench; 7.0 ed.; Stewart and Associates, Inc., 1997.
(25) Carey, F. A.; Sundberg, R. J. *Advanced Organic Chemistry, Part A: Structure and Mechanisms*, 3rd ed.; Plenum: New York, 1990.
(26) Morrison, R. T.; Boyd, R. N. *Organic Chemistry*, 3rd ed.; Allyn and Bacon: Boston, 1973.
(27) de la Mare, P. B. D.; Hassan, M. *J. Chem. Soc.* **1958**, *1958*, 1519.
(28) Stock, L. M.; Himoe, A. *J. Am. Chem. Soc.* **1961**, *83*, 1937.